JOURNAL OF SOLID STATE CHEMISTRY 63, 23–30 (1986)

High-Temperature Behavior of $CoAs_2$ and $CoSb_2$

T. SIEGRIST[1] AND F. HULLIGER

Laboratorium für Festkörperphysik ETH, CH-8093 Zürich, Switzerland

Received July 22, 1985; in revised form October 7, 1985

The arsenopyrite–marcasite-type transformation of $CoAs_2$ and $CoSb_2$ has been studied by magnetic, electrical, and calorimetric measurements. The transition is clearly detectable on the differential scanning and susceptibility curves whereas the resistivity curves show only a smeared transition which does not lead to a distinctly metallic type. The room-temperature structure of $CoSb_2$ has been refined on single crystals.

I. Introduction

Quite a series of papers have been published on the chemical bonding in arsenopyrites and marcasites (*1–18*). The monoclinic arsenopyrite (FeAsS) structure is met as the room-temperature modification of transition-element pnictides TX_2 where the transition element T has a formal d^5 electron configuration. TX_2 pnictides as well as some chalcogenides with a d^6 configuration crystallize in the normal marcasite FeS_2 structure which is characterized by axial ratios $c/a = 0.73 \cdots 0.75$ and $c/b = 0.61 \cdots 0.63$. The TX_2 pnictides of the loellingite branch with formal configuration d^4 or d^2 crystallize in a compressed marcasite version ($c/a = 0.53 \cdots 0.57$ and $c/b = 0.47 \cdots 0.50$). These structures can be derived by small atomic displacements from a hypothetical $(M\square)X_2$ defect NiAs-type structure with ordered vacancies (□) between all X layers. From this archetype nature also derived the rutile TiO_2, the $CaCl_2$, and the MnO(OH) structures.

The *c*-axis is rather short in the loellingite branch (it corresponds to the *c*-axis in rutile) suggesting M-chain formation. In the arsenopyrites the monoclinic deformation of the marcasite cell is accompanied by the formation of M–M "pairs," i.e., short and long distances alternate within the metal chains. Since the cations are crystallographically equivalent we cannot think of a mixture of d^4 and d^6 cations although the arsenopyrite structure can be composed of alternating layers of marcasite and loellingite type (*14*). The lowered symmetry induces a doubling of the unit cell and a splitting of the singly occupied *d*-subband. The resulting lower band is filled with the two lone *d*-electrons per pair. According to more sophisticated modern views it is primarily the different deformation of the $[MX_{6/2}]$ octahedra of these chains that induces the appropriate splitting of the subbands, but not the M–M interaction. Whatever the reason for this band splitting is, a transition from the arsenopyrite to the mar-

[1] Present address: Solid State Chemistry, Chemistry Division, NRCC, Ottawa, K1A OR9 Canada.

0022-4596/86 $3.00

casite structure is expected to induce a semiconductor–metal transition, reminiscent of a Peierls transition and analogous to the transition in VO_2 and NbO_2. It was our goal to verify this change in the electronic character of $CoAs_2$ and $CoSb_2$. In fact we even intended to verify the charge-density wave transitions predicted by Tosati (*19*) to occur in doped or alloyed phases like Co $Sb_{2-x}Te_x$ at much lower temperatures than in the pure pnictides. However, we had to abandon this project as we did not succeed in growing appropriate single crystals.

II. Experimental

Small single crystals of $CoAs_2$ and $CoSb_2$ with well-defined faces have been prepared by a transport reaction below the peritectic temperature. We used a closed silica tube as container and chlorine or iodine as transport agents. We started either from sintered material or directly from the elements. The size of the crystals obtained was well appropriate for crystallographic measurements but at the lower limit for four-probe resistivity measurements. The electrical measurements were carried out in an open vacuum of 10^{-5} Torr which reduces the reliability of the measurements somewhat due to partial dissociation or contamination of the crystals at high temperatures. For the current leads and the voltage probes we used molybdenum wires pressed onto the sample. The chromel–alumel thermocouple for the temperature control was in loose contact with the sample.

The magnetic susceptibility was measured between room temperature and about 1000 K with a Faraday balance in an external field of 4.5 kOe. Several nonoriented single crystals were sealed in a thin-walled quartz ampoule. The empty quartz container was measured afterwards in the same temperature range. The Pt/Pt-Rh thermocouple was mounted directly below the ampoule. $HgCo(SCN)_4$ was used for calibration. The temperature range was limited by the reaction of cobalt with silica, which leads to strongly paramagnetic blue silicates.

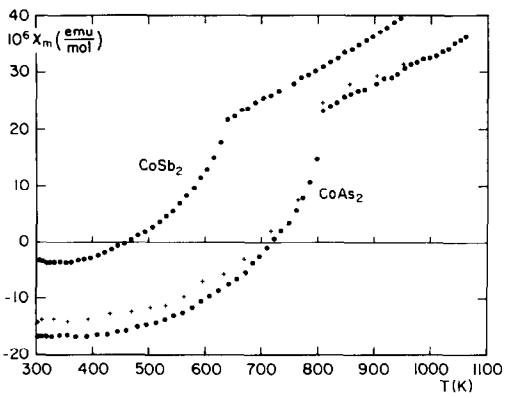

FIG. 1. Temperature dependence of the magnetic susceptibility of $CoAs_2$ and $CoSb_2$ (several nonoriented single crystals of batch 3 and 28, respectively). Dots: rising temperature; crosses: decreasing temperature.

The phase transition was studied by differential scanning calorimetry. The experiments were carried out under an inert atmosphere with a Perkin–Elmer DSC-2C calorimeter at scanning rates of 5 and 10 deg/min, using crystals of 4–5 mg weight sealed under argon in gold containers. Three runs were made in each direction on one sample of $CoAs_2$ and two different samples of $CoSb_2$.

III. Results of the Physical Measurements

The most satisfactory results were obtained from the magnetic measurements. The temperature variation of the susceptibility of $CoAs_2$ and $CoSb_2$ is shown in Fig. 1. The curves are reminiscent of those for $\Delta\beta'(T)$ (*14*), where $\Delta\beta'$ is the deviation from 90° of the monoclinic angle in the pseudomarcasite cell ($\Delta\beta' = 0$ above the transition; see below). The character of the curves points to a second-order transition. No jump is detectable within our experimental resolution.

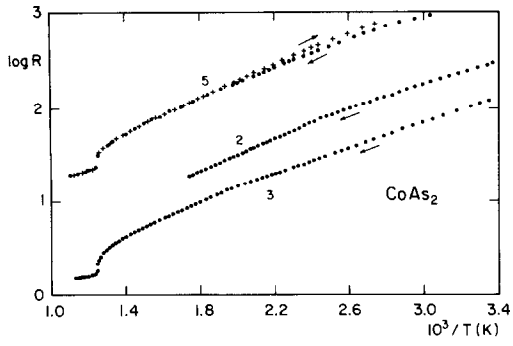

FIG. 2. Temperature dependence of the resistivity of three different $CoAs_2$ single crystals of unknown orientation. Arbitrary R units, since the geometrical factor remained undetermined.

The thermal-scanning experiments, on the other hand, revealed a rather sharp peak at least in the case of $CoAs_2$. The thermal effect is restricted to a temperature range of 3–5 K. The enthalpy change $-\Delta H$ amounts to about 800 J/mol for $CoAs_2$ and is roughly an order of magnitude smaller in $CoSb_2$ (~100 J/mol). From the different runs we derive the following transition temperatures and entropy changes:

$CoAs_2$: $T_{tr} = 800 \pm 2$ K (heating), 797 ± 2 K (cooling)

$$\Delta S \approx 1 \text{ J/mol} \cdot \text{K}$$

$CoSb_2$: $T_{tr} = 644 \pm 2$ K (heating and cooling)

$$\Delta S \approx 0.17 \text{ J/mol} \cdot \text{K}$$

Our transition temperature for $CoSb_2$ is in fair agreement with the value 650 K reported by Kjekshus and Rakke (*14*).

As was to be expected for semiconducting material not especially purified, the resistivity data obtained for $CoAs_2$ and $CoSb_2$ are much less satisfactory. Since only a few of our crystals were large enough for the four-probe measurements we had little chance to evaluate the intrinsic properties, particularly in the case of $CoSb_2$ where the influence of the diminishing distortions on the energy gap is expected to be noticeable above 450 K. Some of our measurements are reproduced in Figs. 2 and 3. Assuming a temperature dependence $\log \rho \sim \Delta E/2kT$, we derive a gap $\Delta E \approx 0.3$ eV for $CoAs_2$. The increase of the slope of $\log \rho$ above 500 K may already be due to the nonlinear decrease of the gap as a consequence of the gradual transition to the marcasite structure. From the resistivity curves we estimate a transition temperature $T_{tr} = 804 \pm 4$ K for both $CoAs_2$ crystals measured. The resistivity jump extrapolated from 500 K amounts only to a factor of about 2, but what is even more intriguing, the resistivity behavior of the marcasite phase is far from being distinctly metallic. The situation is even worse in the case of $CoSb_2$. Unfortunately most of our $CoSb_2$ crystals were obviously so impure or off-stoichiometric that they showed impurity-band conduction up to the transition temperature. The three crystals which revealed a semiconductor-like behavior unfortunately decomposed at high temperatures before we were able to confirm the upward curve on cooling. We deduce a gap $\Delta E \approx 0.17$ eV in the temperature range 450–600 K which compares with 0.2 eV derived by Dudkin and Abrikosov

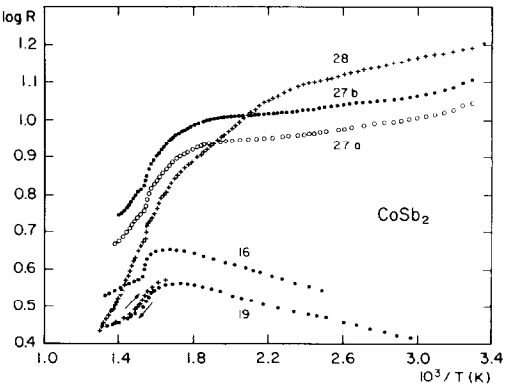

FIG. 3. Temperature dependence of the resistivity of various $CoSb_2$ single crystals of unknown orientation. Arbitrary R units; roughly mΩ cm units for samples 27 and 28.

(*20*) from 550 to 800 K, i.e., across the arsenopyrite–marcasite transition.

It is noteworthy that all our arsenide samples (crystals and sintered material) as well as sintered CoAsSb, were of *n*-type with room-temperature Seebeck coefficients of about −200 and −180 μV/K, respectively, whereas all $CoSb_2$ samples were of *p*-type ($S \approx 40$ μV/K). As expected a polycrystalline sample of $CoSb_{1.9}Te_{0.1}$ again showed *n*-type conduction ($S \approx -80$ μV/K).

IV. Discussion of the Physical Measurements

Whereas our experimental findings do not show much relation to VO_2 the similarity with NbO_2 is evident. NbO_2 has a larger energy gap than the cobalt dipnictides as well as a higher transition temperature (~1080 K) but several of the published resistivity curves (*21–25*) are rather similar to ours, i.e., they simulate a semiconductor behavior also in the high-symmetry modification. Other authors (*26, 27*), however, detected a distinct semiconductor–metal transition, whereby Bélanger *et al.* (*27*) on single crystals found metallic conductivity only along the *c*-axis of the rutile phase, but semiconductivity perpendicular to it.

A similarity between NbO_2, $CoAs_2$, and $CoSb_2$ is met also in the magnetic susceptibility (above 700 K for NbO_2). The susceptibility of NbO_2 also increases almost linearly above the transition (*21*). This slight increase above T_{tr} proves the band-like behavior. For a marcasite-type phase with a localized d^5 configuration ($\sim t_{2g}^5$) we would expect a decrease according to a Curie–Weiss dependence.

The specific-heat anomaly of NbO_2, on the other hand, is much more pronounced and extends over about 100 K, as is expected for a second-order transition. Since in $CoAs_2$ and $CoSb_2$ the main thermal effect occurs within a few degrees, it well might be that the last step of the transition is discontinuous in the pnictides. The fact that the transition in $CoSb_2$ is even less pronounced than in $CoAs_2$ may be explained by structural arguments. In the structure of $CoAs_2$ the equal distance between the Co atoms of 3.126 Å splits into the two values of 2.78 and 3.476 Å. In the case of $CoSb_2$, the corresponding values are 3.377 Å for the equal, 3.03 and 3.73 Å for the short and the long distance, respectively. If we assume that the overlap of the *d*-wave functions determines the strength of the phase transition, then a much larger effect is indeed expected for the arsenide.

V. The Crystal Structure of $CoSb_2$ at 295 K

The single crystal chosen for the structure determination had an irregular prismatic shape of approximate dimensions $0.25 \times 0.10 \times 0.16$ mm^3. Precession patterns proved the diffraction symmetry to be $2/m$, and the systematic absences led to space group $P2_1/c$ in agreement with literature data (*14*). The lattice constants given in Table I were calculated from 25 reflections measured on a Guinier–Jagodzinski camera with Cu$K\alpha_1$ radiation and silicon ($a = 5.43047$ Å) as internal standard. The intensities for the structure determination were collected on a SYNTEX $P2_1$ automatic four-circle diffractometer with monochromatized Mo$K\alpha$ radiation ($\lambda_{MoK\bar{\alpha}} = 0.71069$ Å). The intensities were measured by the $\theta - 2\theta$ scan method. A number of 2291 reflections was collected in the range $\sin\vartheta/\lambda \leqq 0.8$ ($2\vartheta \leqq 70°$) yielding 1152 independent reflections of which 1087 were greater than 3σ. The intensities were corrected for absorption ($\mu_{MoK\alpha} = 300$ cm^{-1}) by the Gaussian integration method. The shape of the crystal was approximated by 11 faces measured with a high-resolution telescope on the diffractometer. All calculations were carried out with the XRAY-

TABLE I

STRUCTURAL DATA FOR $CoSb_2$ AT 295 K: ARSENOPYRITE STRUCTURE, SPACE GROUP $P2_1/c$ (No. 14), PEARSON SYMBOL mP 12. a = 6.5051(6), b = 6.3833(5), c = 6.5410(6) Å, β = 117.65(1)°; V = 240.59 Å^3, d_x = 8.353 g/cm^3[a]

	x	y	z	U_{11}	U_{22}	U_{33}	U_{12}	U_{13}	U_{23}
Co	0.2701(3)	−0.0005(3)	0.2817(3)	1.62(8)	2.19(8)	1.71(8)	0.5(5)	0.69(6)	0.06(6)
Sb(1)	0.3466(2)	0.3569(2)	0.1675(2)	1.67(5)	2.15(5)	1.79(5)	−0.08(3)	0.74(3)	0.05(3)
Sb(2)	0.1489(2)	0.6393(2)	0.3671(2)	1.63(5)	2.18(5)	1.78(5)	−0.03(3)	0.68(3)	0.04(3)

[a] All atoms in 4(c): $\pm(x, y, z; x, \frac{1}{2} - y, \frac{1}{2} + z)$.

System 72 (*28*). As starting parameters for the refinement we used the data given by Zhdanov and Kuz'min (*29*). For the full-matrix least-squares refinement 865 reflections in the range $0.5 \leqq \sin\vartheta/\lambda \leqq 0.8$ were used, which led to an R-value of 0.078. A further isotropic extinction correction reduced the final R-value to 0.054.

The results of our structure determination are collected in Tables I and II. Table I shows the structural and thermal parameters while the interatomic distances and angles are listed in Table II. The distortions of the octahedral coordination of the cobalt atoms and of the tetrahedral coordination of the antimony atoms are evident from the

TABLE II

INTERATOMIC DISTANCES (IN Å UNITS) UP TO 3.47 AND 4.0 Å FOR Sb AND Co, RESPECTIVELY, AND BOND ANGLES (IN DEGREES) IN $CoSb_2$

$Co^{(0)}$–$Sb(1)^{(6)}$	2.508(4)	$Sb(1)^{(0)}$–$Co^{(7)}$	2.508(4)	$Sb(2)^{(0)}$–$Co^{(1)}$	2.575(3)		
$Sb(1)^{(0)}$	2.521(3)	$Co^{(0)}$	2.521(3)	$Co^{(10)}$	2.591(7)		
$Sb(1)^{(9)}$	2.527(3)	$Co^{(8)}$	2.527(3)	$Co^{(6)}$	2.603(5)		
$Sb(2)^{(2)}$	2.575(3)	$Sb(2)^{(0)}$	2.858(4)	$Sb(1)^{(0)}$	2.858(4)		
$Sb(2)^{(11)}$	2.591(7)	$Sb(2)^{(3)}$	3.28(2)	$Sb(1)^{(3)}$	3.28(2)		
$Sb(2)^{(7)}$	2.603(5)						
$Co^{(4)}$	3.03(2)						
$Co^{(5)}$	3.73(2)						
$Sb(1)^{(0)}$–$Co^{(0)}$–$Sb(2)^{(2)}$	174.19(8)	$Co^{(0)}$–$Sb(1)^{(0)}$–$Co^{(7)}$	130.89(8)	$Co^{(1)}$–$Sb(2)^{(0)}$–$Co^{(6)}$	123.70(7)		
$Sb(1)^{(9)}$	92.67(9)	$Co^{(8)}$	127.26(8)	$Co^{(10)}$	126.93(7)		
$Sb(2)^{(7)}$	90.31(8)	$Co^{(7)}$–$Sb(1)^{(0)}$–$Co^{(8)}$	73.96(7)	$Co^{(6)}$–$Sb(2)^{(0)}$–$Co^{(10)}$	91.80(8)		
$Sb(1)^{(6)}$	89.61(7)	$Sb(2)^{(0)}$–$Sb(1)^{(0)}$–$Co^{(8)}$	109.78(7)	$Sb(1)^{(0)}$–$Sb(2)^{(0)}$–$Co^{(10)}$	103.25(7)		
$Sb(2)^{(11)}$	83.97(7)	$Co^{(7)}$	107.93(7)	$Co^{(6)}$	106.16(7)		
$Co^{(4)}$	91.90(7)	$Co^{(0)}$	104.06(8)	$Co^{(1)}$	102.48(8)		
$Co^{(5)}$	86.03(6)						
$Sb(1)^{(6)}$–$Co^{(0)}$–$Sb(2)^{(7)}$	174.46(9)	where the symmetry operations are:					
$Sb(1)^{(9)}$	106.04(7)	(0) x, y, z	(1) $x, 1 + y, z$	(2) $x, -1 + y, z$	(3) $1 - x, 1 - y, 1 - z$		
$Sb(2)^{(11)}$	86.27(8)	(4) $1 - x, -y, 1 - z$	(5) $-x, -y, -z$	(6) $x, \frac{1}{2} - y, \frac{1}{2} + z$			
$Sb(2)^{(7)}$–$Co^{(0)}$–$Sb(2)^{(11)}$	88.20(6)	(7) $x, \frac{1}{2} - y, -\frac{1}{2} + z$	(8) $1 - x, \frac{1}{2} + y, \frac{1}{2} - z$	(9) $1 - x, -\frac{1}{2} + y, \frac{1}{2} - z$			
$Sb(1)^{(9)}$	79.50(8)	(10) $-x, \frac{1}{2} + y, \frac{1}{2} - z$	(11) $-x, -\frac{1}{2} + y, \frac{1}{2} - z$				
$Sb(1)^{(9)}$–$Co^{(0)}$–$Sb(2)^{(11)}$	167.25(9)						
$Co^{(4)}$–$Co^{(0)}$–$Co^{(5)}$	175.56(9)						

Note. The uncertainty of the last digit is added in parentheses.

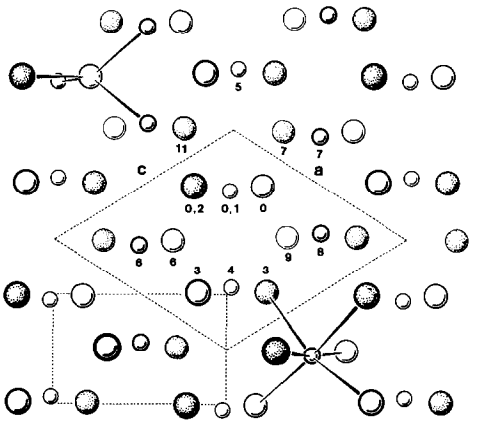

FIG. 4. The monoclinic arsenopyrite structure of $CoSb_2$(r) projected onto the (a,c) plane. The frame of the orthorhombic marcasite cell of the high-temperature modification is indicated below. The numbers given refer to the symmetry operations defined in Table II.

deviations of the angles from 90° (180°) and 109.48°, respectively (compare Fig. 4. The numbers given refer to the symmetry operations defined in Table II). An ideal octahedral and tetrahedral coordination is not possible in the marcasite structure either, but the distortions in the monoclinic form are enhanced by the pair formation in the Co chains, or by the asymmetry of the Co–Sb bonds (the Co–Sb(1) distances are distinctly shorter than the Co–Sb(2) distances!).

Comparing the positional parameters given by Zhdanov and Kuz'min (*29*) with our data, we notice only one major difference: our value for the x position of Sb(2) is 0.1489(2) instead of their value 0.162(3). This leads to a more even distribution of the distances between the atoms.

VI. Crystal-Chemical Reflections

The distortions in the arsenopyrite structure require a doubling of the original marcasite unit cell. The standard monoclinic arsenopyrite cell evolves from the orthorhombic marcasite cell by the transformation

$$\vec{a}_{mon} = \vec{a}_{orth} + \vec{c}_{orth}$$
$$\vec{b}_{mon} = \vec{b}_{orth}$$
$$\vec{c}_{mon} = -\vec{a}_{orth} + \vec{c}_{orth}$$

and a shift of the origin by (0, 0, $-\frac{1}{2}$). If we describe the orthorhombic marcasites in the twice as large arsenopyrite cell, then the monoclinic angle β is 106.6 · · · 106.9° for the ordinary marcasites with d^6 configuration ($NiAs_2$ and $NiSb_2$), near 118° for the "d^4/d^6 mixtures" $FeNiAs_4$ and $FeNiSb_4$, and between 120.45° (OsP_2) and 123.77° ($RuSb_2$) for the loellingites with "d^4" and d^2 configuration, compared to β = 111 · · · 114° for the ternary arsenopyrites and 111.5 · · · 118° for the binary arsenopyrites.

Vice versa a marcasite-related arsenopyrite cell can be defined as in Ref. (*14*) with $\beta' = 90 + \Delta\beta'$, where $\Delta\beta'$ is a measure of the distortion. The deformation $\Delta\beta'$ of the pseudomarcasite cell (for $CoSb_2$ $\Delta\beta'$ = 0.356°) is obviously larger the higher the transition temperature is (*14*). Since almost no structure refinements were performed on ternary arsenopyrites we tried to correlate the pair formation with the cell distortion, which is known. In Fig. 5 we have plotted in a logarithmic scale the ratio of the long (T · · · T) to the short (T–T) cation distance as a function of $(c - a)/(a + c)$. A similar dependence is obtained if we use $\log(\Delta\beta')$ as the argument instead of $\log(c - a)/(a + c)$ since in a good approximation

$$\Delta\beta'(°) \approx 0.1235\ (c - a)/(a + c),$$

although the exact relation between $\Delta\beta'$ and a, c, β is given by

$$\sin(\Delta\beta') = (c^2 - a^2)\ [(a^2 + c^2)^2 - 4a^2c^2\cos^2\beta]^{-1/2}.$$

As one of the referees pointed out the somewhat poor linear relationship is not very exciting. Nevertheless it visualizes

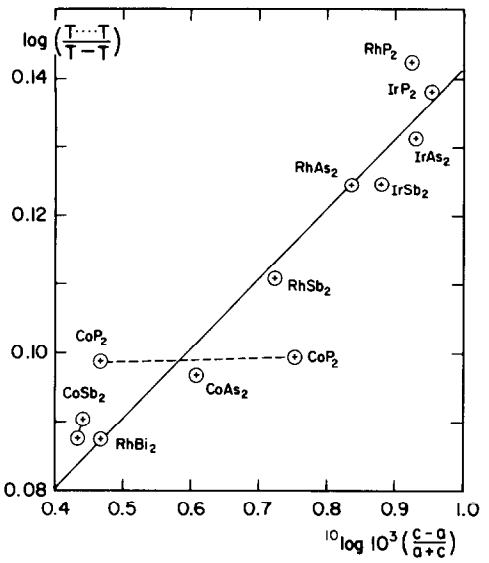

FIG. 5. The ratio of the long to the short metal–metal distance vs $(c - a)/(a + c)$ of the monoclinic unit cell of the binary arsenopyrite-type pnictides. Logarithmic scales; data from literature (*30*); two sets for CoP_2 and $CoSb_2$ from different source.

how in the binary arsenopyrite representatives the distortion decreases on replacing the anion in the sequence P → As → Sb → Bi, as well as in the cation sequence $5d \rightarrow 4d \rightarrow 3d$. In the ternary arsenopyrites this regularity is not observed. This surprising fact may partly be due to deviations from the exact 1 : 1 anion stoichiometry. From published unit-cell data (*30*) we conclude that the strongest distortions do not occur in OsPS but in OsAsSe and FeAsSe, while for FePS, FeSbS, FeAsTe, and RuSbS the distortions are very weak. As a consequence the monoclinic–orthorhombic transformation should take place at very low temperatures in these latter compounds. In FePS, however, no transition was detectable up to ~780 K (*31*) while a transition temperature of about 550 K is deduced from the diagram given by Kjekshus and Rakke (*14*) for the binary pnictides. Based on the cell distortion the transition in FeAsSe might be expected near 1500 K, so that it is not surprising that resistivity measurements revealed no anomaly up to 830 K (*31*). FeAsS too must remain monoclinic to well above 720 K (*31*), and on a sintered sample of RuSbSe, for which the room-temperature deformation suggests a transition near 800 K, we did not detect any anomaly up to 700 K. Thus it is obvious that the arsenopyrite family still offers quite a series of problems to be solved.

Acknowledgments

We thank Professor Erio Tosatti (Trieste) for his stimulating interest and apologize for our failure in growing the strongly doped crystals required to confirm his predictions about the charge-density waves. Moreover, we are indebted to Professor H. C. Siegmann and the Swiss National Science Foundation for support. The DSC data were taken during a stay of T.S. at the IBM Watson Research Center, Yorktown Heights.

References

1. F. HULLIGER AND E. MOOSER, *in* "Progress in Solid State Chemistry" (H. Reiss, Ed.), Vol. 2, p. 330, Pergamon, New York (1965).
2. W. B. PEARSON, *Z. Kristallogr.* **121,** 449 (1965).
3. F. HULLIGER, *in* "Structure and Bonding" (C. K. Jørgensen *et al.*, eds.), Vol. 4, p. 83, Springer, Berlin (1968).
4. E. H. NICKEL, *Canad. Mineral.* **9,** 311 (1968).
5. G. BROSTIGEN AND A. KJEKSHUS, *Acta Chem. Scand.* **24,** 2993 (1970).
6. A. KJEKSHUS, *Acta Chem. Scand.* **25,** 411 (1971).
7. A. KJEKSHUS AND D. G. NICHOLSON, *Acta Chem. Scand.* **25,** 866 (1971).
8. J. B. GOODENOUGH, *J. Solid State Chem.* **5,** 144 (1972).
9. A. KJEKSHUS, T. RAKKE, AND A. F. ANDRESEN, *Acta Chem. Scand. Ser. A* **28,** 996 (1974).
10. A. KJEKSHUS AND T. RAKKE, *Acta Chem. Scand. Ser. A* **28,** 1001 (1974).
11. M. E. FLEET, *Z. Kristallogr.* **142,** 332 (1975).
12. W. JEITSCHKO AND P. C. DONOHUE, *Acta Crystallogr. Sect. B* **31,** 574 (1975).
13. A. KJEKSHUS, T. RAKKE, AND A. F. ANDRESEN, *Acta Chem. Scand. Ser. A* **31,** 253 (1977).
14. A. KJEKSHUS AND T. RAKKE, *Acta Chem. Scand. Ser. A* **31,** 517 (1977).

15. J. A. TOSSELL, D. J. VAUGHAN, AND J. K. BURDETT, *Phys. Chem. Minerals* **7,** 177 (1981).
16. J. K. BURDETT AND T. J. MCLARNAN, *Inorg. Chem.* **21,** 1119 (1982).
17. S. D. WIJEYESEKERA AND R. HOFFMANN, *Inorg. Chem.* **22,** 3287 (1983).
18. W. JEITSCHKO, U. FLÖRKE, AND U. D. SCHOLZ, *J. Solid State Chem.* **52,** 320 (1984).
19. E. TOSATTI, ICTP Trieste, private communication (1978).
20. L. D. DUDKIN AND N. KH. ABRIKOSOV, *Russ. J. Inorg. Chem.* **2,** 325 (1957).
21. K. SAKATA, *J. Phys. Soc. Japan* **26,** 867 (1969).
22. R. F. JANNINCK AND D. H. WHITMORE, *J. Phys. Chem. Solids* **27,** 1183 (1966).
23. K. SETA AND K. NAITO, *J. Chem. Thermodyn.* **14,** 921 (1982).
24. J. M. GALLEGO AND C. B. THOMAS, *Solid State Commun.* **43,** 547 (1982).
25. J. A. ROBERSON AND R. A. RAPP, *J. Phys. Chem. Solids* **30,** 1119 (1969).
26. C. N. R. RAO, G. RAMA RAO, AND G. V. SUBBA RAO, *J. Solid State Chem.* **6,** 340 (1973).
27. G. BÉLANGER, J. DESTRY, G. PERLUZZO, AND P. M. RACCAH, *Canad. J. Phys.* **52,** 2272 (1974).
28. J. M. STEWART, G. J. KRUGER, H. L. AMMON, C. DICKINSON, AND S. R. HALL, X-RAY System 72, Tech. Rept. TR-192, 1972 (Computer Science Center, Univ. of Maryland, College Park, Md.); extended by D. Schwarzenbach, Univ. of Lausanne.
29. G. S. ZHDANOV AND R. N. KUZ'MIN, *Sov. Phys.–Crystallogr.* (*Engl. Transl.*) **6,** 704 (1962).
30. LANDOLT-BÖRNSTEIN, Numerical Data, New Series, Group III, Vol. 17g, p. 119, Springer, Berlin (1984).
31. F. HULLIGER, *Helv. Phys. Acta* **32,** 615 (1959).